1 # Title:

2 Development of a new genotype–phenotype linked antibody screening system

3 # Authors:

4 Takashi Watanabe[1*], Hikaru Hata[2], Yoshiki Mochizuki[1], Fumie Yokoyama[1], Tomoko

5 Hasegawa[1], Naveen Kumar[3], Tomohiro Kurosaki[2,4], Osamu Ohara[1,5] and Hidehiro

6 Fukuyama[2,6,7]

7 # Affiliations:

8 [1]Laboratory for Integrative Genomics, RIKEN Center for Integrative Medical Sciences,

9 Yokohama, 230-0045, Japan

10 [2]Laboratory for Lymphocyte Differentiation, RIKEN Center for Integrative Medical Sciences,

11 Yokohama, 230-0045, Japan

12 [3]Laboratory for Integrated Bioinformatics, RIKEN Center for Integrative Medical Sciences,

13 Yokohama, 230-0045, Japan

14 [4]Laboratory of Lymphocyte Differentiation, WPI Immunology Frontier Research Center,

15 Osaka University, Osaka, 565-0871, Japan

16 [5]Department of Applied Genomics, Kazusa DNA Research Institute, Chiba 292-0818, Japan

17 [6]Division of Immunology, Near-InfraRed Photo-Immunotherapy Research Institute, Kansai

18 Medical University, Hirakata, Osaka,573-1010, Japan

19 [7]INSERM EST, Strasbourg Cedex 2, 67200, France

20 *To whom correspondence should be addressed. Tel: +81 45 503 9696; Fax: +81 45 503

21 9694; Email: twatanabe@riken.jp

22 Impact Statement:

23 A Golden Gate-based dual-expression vector enables rapid screening, which facilitates

24 efficient isolation of high-affinity cross-reactive antibodies for therapeutic or diagnostic use

25 and provides a crucial advance for pandemic preparedness.

26 Keywords:

27 Membrane-bound Ig expression, NGS-based Ig-seq, Golden Gate Cloning, influenza

28 broadly-reactive

29

Abstract:

Antibodies are powerful tools for the therapy and diagnosis of various diseases. In addition to conventional hybridoma-based screening, recombinant antibody-based screening has become a common choice; however, its application is hampered by two factors: 1) screening starts after Ig gene cloning and recombinant antibody production only, and 2) the antibody is composed of paired chains, heavy and light, commonly expressed by two independent expression vectors. Here, we introduce a method for the rapid screening of recombinant monoclonal antibodies by establishing a Golden Gate-based dual-expression vector and *in-vivo* expression of membrane-bound antibodies. Using this system, we demonstrate the rapid isolation of influenza cross-reactive antibodies with high affinity from immunized mice within 7 days. This system is particularly useful for isolating therapeutic or diagnostic antibodies, e.g., during foreseen pandemics.

43 # Introduction:

44 Technical improvements in the rapid isolation of monoclonal antibodies (mAbs) are critical
45 for the diagnostic and therapeutic development of such antibodies. This need became
46 apparent to the general public during the COVID-19 pandemic. Antibodies isolated from
47 convalescent COVID-19 patients are valuable resources for the development of mAb
48 therapeutics and rapid diagnostic tools. Human antibodies can be administered to other
49 patients without the need to humanize in an emergency and with a slight modification of
50 Fc receptor binding (1) to increase the half-life or reduce the risk of antibody-dependent
51 enhancement. Although production costs remain high, the efficiency of generating
52 recombinant antibodies has dramatically improved with the use of mammalian cell lines,
53 and the application of therapeutic antibodies is likely to expand in the near future (2).

54 The gold standard method for isolating mAbs is the hybridoma technology developed
55 by Kohler and Milstein in 1975 (3), in which antibody-producing B cells are fused with
56 immortal B cells, called myelomas, to produce long-lasting antibody-producing B cells. In
57 addition to hybridoma technology, new methods have been developed to increase mAb
58 screening efficiency. These include direct immortalization of B cells by gene
59 reprogramming using the Epstein–Barr virus (4) or retrovirus-mediated gene transfer (5),
60 cloning of variable region-encoding genes by single-cell PCR (6,7), single-cell culture

61 screening (8), and *in-vitro* screening of recombinant antibody libraries (9–13). Some of
62 these methods have successfully yielded high-affinity antibodies in various formats,
63 including single variable domain on a heavy chain or single-chain fragment variable
64 antibodies. Although hybridoma technology is highly reliable for the isolation of valuable
65 antibodies from animal models, such as mice, rats, and hamsters, it is time-consuming
66 and requires technical skill. The development of a new fusion partner cell line, SPYMEG,
67 has enabled the production of human hybridomas and opened a new direction for the
68 isolation of human mAbs (14). Although many of these new technologies have increased
69 the throughput for mAb isolation, the procedure still requires significant resources and
70 time.

71 To dramatically enhance the efficiency of mAb isolation, we used next-generation
72 sequencing (NGS) technology, which has revolutionized the sequencing of immunoglobulin
73 (Ig) variable-region genes. For instance, tens of thousands of Ig genes specific to certain
74 antigens can be identified by combining droplet-based single-cell isolation with DNA
75 barcode antigen technology, followed by NGS (15). Although Ig genes can be sequenced
76 at high throughput, there is no method for screening antibodies in a high-throughput
77 format that is compatible with NGS technology.

78 In this study, we developed a new functional screening method that is compatible
79 with NGS to rapidly identify antigen-specific clones. We first generated an Ig dual-
80 expression vector using Golden Gate Cloning (16), which enabled the linkage of heavy-
81 chain variable and light-chain variable DNA fragments obtained from a single-sorted B cell,
82 followed by the expression of membrane-bound Ig. This single-step procedure enabled the
83 enrichment of antigen-specific, high-affinity Igs by flow cytometry, which is significantly
84 faster than conventional cloning-based methods that require sequential steps. To
85 demonstrate the efficiency of our new method, we screened for potent broadly reactive
86 antibodies (17–19) against the influenza virus in an experimental mouse model using our
87 technology. Broad reactivity antibodies allow for the development of influenza vaccines
88 that are effective across seasonal variations in influenza strains, which can only be
89 accomplished by screening a large number of candidate antibodies. We first raised cross-
90 reactive B cells against various hemagglutinin (HA) antigens from the influenza virus by
91 sequential immunization with heterotypic HA antigens from group 1 influenza. Using this
92 technology, we obtained several mAbs that bind to other group 1 HA antigens, and even
93 to group 2 HA antigens, of the influenza virus. Our technology can also be applied to
94 human antibody screening and represents a new line of mAb screening that accelerates
95 the isolation of therapeutic and diagnostic mAbs.

96 # Results:

97 ## Rapid membrane-bound dual Ig expression screening system

98 Cloning-based Ig screening involves several steps: cloning two Ig gene fragments that
99 encode heavy and light chains independently from a single cell, co-expressing these Ig
100 chains, and purifying individual recombinant antibodies. These steps are labor intensive.
101 We established a new antibody screening system for the isolation of valuable mAbs
102 (details in the methods). Eventually, the antigen-binding Ig transformants were collected
103 by sorting in a bulk fashion, and the unique CDR3 region and clones of interest were
104 identified using the Ig-seq database (Fig. 1A).

105 We generated a dual-expression vector to express both Ig heavy and kappa/lambda
106 in a single-expression vector (Fig. 1B). These plasmids were individually transfected
107 transiently to the floating human FreeStyle 293 cell line. Igs were expressed on the cell
108 surface within 2 days, and their expression could be confirmed and normalized by *Venus*
109 (20) expression since the Ig heavy chain is fused with *Venus* at the cytoplasmic domain
110 tail (Fig. 1C). The advantage of this system is the rapid enrichment of clones of interest
111 through bulk screening. In the current single-cell-based cloning/screening, plasmid DNA
112 extracted from the collected antigen-binding bulk transformants is sequenced for the
113 heavy chain CDR3 region. The CDR3 region is unique and can be used for the identification

114 of a clone (21,22). This membrane-bound Ig expression system links antigen-binding

115 features and genetic information of the Ig repertoire.

116 Building the Ig-seq database and analysis

117 As a model experiment, we obtained broadly reactive antibodies against influenza viruses

118 using multiple HA probes. We prepared two HA proteins as probes: A/Puerto Rico/8/1934

119 (H1N1), designated as PR8, and A/Okuda/1957 (H2N2), designated as H2. A total of 374

120 IgG1^{+} B cells of either PR8^{+} (204 cells), H2^{+} (99 cells), or PR8^{+}H2^{+} (71 cells) were

121 collected in a single-cell fashion. We obtained sequences of 284 independent clones. The

122 success rate of cloning the paired Ig fragments was 75.9%. An overview of heavy chain V-

123 D-J and light chain V-J usage and repertoire clonality is shown in Supplementary Fig. 1A

124 and B. Mutation rates and CDR3 lengths of the heavy chains of the three cell populations

125 (PR8^{+}, H2^{+}, and PR8^{+}H2^{+}) were comparable (Supplementary Fig. 1C and D). These

126 results indicate that broadly reactive antibodies do not require unique genetic traces to

127 obtain breadth in our experimental setup.

128 Isolation of H2- and H1-reactive B cells

129 On day 2 after transfection of individual 284 clones, the transformants were mixed and

130 stained with HA probes (Fig. 2A). As shown in Fig. 2B, we selected three prominent

131 populations, H1^{+}H2^{+} (cross), H2^{+} (H2), and H1^{+} (H1), and collected them in bulk. In

132 contrast to bacterial transfection, mammalian cell lines, such as FreeStyle 293 cells, can

133 contain multiple plasmids in a cell and ectopically express multiple proteins. Therefore, we
134 decided to mix the transformants instead of plasmids. We sorted a total of 2,981 cells,
135 classified into three strong binder populations, and performed sequencing (Fig. 2B). These
136 bulk Ig-seq data are referred to as Ig-seq data, as described above. A total of 190 clones
137 from the three populations were verified for their sequences and HA binding by flow
138 cytometry analysis, as shown in Fig. 2C; 110 “H1^{+},” 67 “H2^{+},” and 13 “cross” clones were
139 successfully isolated. In parallel, all the transformants were examined individually for
140 comparison with the bulk method. One hundred thirty-eight transformants were verified
141 for their binding to HAs by flow cytometry. Of these, 81 "H1^{+}," 48 "H2^{+}," and 9 "cross"
142 clones were successfully isolated (Fig. 2D). Eight of the 13 "cross" clones obtained in the
143 bulk examination overlapped with “cross" clones obtained in the individual examination
144 (Fig. 2D and E); the binding of one cross clone (D11p4) from the individual examination
145 was so weak that it was not included in the gates sorted in bulk (Fig. 2B). Comparison of
146 the bulk and the individual examinations demonstrated that the rapid bulk method is
147 sufficient for selecting clones of interest.

148 Characterization of “cross” clones for broad reactivity against the influenza virus

149 We decided to further characterize eight common clones between the individual and bulk
150 examinations and one short-ranged clone, D11p4. By generating a secretory form of mAbs
151 for these nine “cross” clones from the individual examination, we characterized their

152 affinity and broadness using six different HA antigens from strains A/Okuda/1957 (H2N2)
153 named for H2, A/Puerto Rico/8/1934 (H1N1) for PR8, A/California/2009 (X-179A) [H1N1]
154 Pdm09 for Cal, A/Texas/50/2012 (X-223) [H3N2] for H3, A/Egypt/N03072/2010(H5N1)
155 for H5, and A/Brisbane/59/2007 [H1N1] (19) for Stem. We determined the affinities (K_d)
156 of the antibodies for the six HA antigens using surface plasmon resonance analysis (Table
157 1 and Supplementary Fig. 2), which ranged from 500 to 100 nM. With the highest affinity
158 among them, the C10p2 antibody bound to Cal at $K_d \simeq 5.66 \times 10^{-10}$ (M). Surprisingly, the
159 antibodies showed a broader spectrum of HA binding among the influenza strains. Seven
160 of the nine mAbs bound to HA from the highly pathogenic avian influenza strain H5N1.
161 Furthermore, six antibodies that bound to H3 were categorized into group 2 (23). In
162 addition, we observed that two of the broadly reactive antibodies recognized the stem
163 region of the HA of A/Brisbane/59/2007. A possible scenario for other stem-negative
164 antibodies is that they may either bind to the stem region of other strains or to the head
165 region of HA. We tested whether some of these antibodies shared features with classic
166 broadly neutralizing antibodies. C179, the first broadly neutralizing mouse antibody
167 isolated in 1993 (17), reacts with the stem region of HAs from group 1 influenza virus
168 strains (23). C179 binds to HAs from group 1 influenza viruses, including H1N1, H2N2,
169 and H5N1. A competition assay for the binding of H2 and PR8 revealed that A6p4
170 competes with C179 (Fig. 3). In addition, our two-dimensional phylogeny map indicated

171 that A6p4 was unique to all clones (Supplementary Fig. 3). Note that we used NSP2 as a
172 negative control antibody, which binds specifically to the HA from A/California/2009 (X-
173 179A) [H1N1] Pdm09 (24). These results demonstrate that we were able to isolate a
174 broadly reactive mAb with an affinity comparable to that of a classic broadly reactive mAb
175 (C179) using our technology.

176 Discussion:

177 The discovery of therapeutic antibodies as well as their demand are increasing (25).
178 Efficiently isolating one biologically significant antibody from the 10^{13} antibody repertoire is
179 challenging. The hybridoma method has long been used for this purpose and remains
180 reliable. However, the fusion rate of B and myeloma cells is < 0.001% in this method;
181 therefore, the number of hybridomas obtained from one individual B cell is limited to
182 several hundred clones, limiting its use in the production of mAbs. As an alternative
183 choice, cloning-based antibody screening has gained popularity, especially for human
184 antibody discovery, because of the lack of a human myeloma cell line similar to that used
185 for murine cell fusion partners. The SPYMEG cell line can generate antigen-specific
186 antibody-producing cells by fusing the murine SP2/0 myeloma cell line and human
187 megakaryoblastic leukemia cell line MEG-01 with human PBMCs (14, 26). In our study, we
188 sorted IgG 1 + B cells. Most of those cross-reactive B cells were memory B cells

189 (Supplementary Figure 4). As shown in Supplementary Figure 5, the cloning efficiency
190 exceeded 75%. Our functional screening by selecting strong binders allowed us to narrow
191 down the number of clones to 13 cross-reactive B cells. One of the clones had a strong
192 affinity of $K_d \simeq 5.66 \times 10^{-10}$ (M). Notably, the generation of antibodies that target regions
193 other than HA cannot be ruled out since the immunization antigen and the detected
194 antigen were the same. However, as shown in Table 1, the cross-reactive antibodies
195 obtained in this study exhibited characteristic binding abilities to each of the six types of
196 HAs. If these were antibodies recognizing His-tag, they would bind to all six types of HA,
197 indicating that these cross-reactive antibodies were no His-specific clones.
198 In addition to gene expression profiling, NGS facilitates antibody repertoire analysis.
199 However, despite breakthroughs in sequencing technology, the process of linking antibody
200 function and its genes is still long and labor intensive. To overcome this issue, we
201 developed a new antibody screening system to directly link antigen–antibody binding (as a
202 function) with a gene encoding the antibody by expressing its membrane-bound form.
203 Among conventional cloning-based mAb isolation methods, this system demonstrates
204 several advantages. 1) Membrane Ig expression can link the antigen-binding feature of
205 membrane-expressed Ig, which can be linked to Ig DNA sequence information using our
206 plasmid construct. Similar to the panning procedure used in phage display (27), antigen-
207 binding cells carry the plasmid encoding Ig genes through surface Ig so that the selection

208 process in bulk format enriches the relevant plasmids for use in further experiments. 2)
209 The dual Ig expression vector links heavy- and light-chain genes, which reduces the
210 plasmid preparation time and stock by half. 3) Highly reliable Golden Gate Cloning
211 technology using type IIs restriction enzymes can readily generate plasmid clones. This
212 reduced the time required to generate an Ig plasmid library. 4) The population profile,
213 defined by the fluorescence intensity during flow cytometry, directly reflected the affinity
214 of a clone (Supplementary Figure 6). Lima et al. developed a dual Ig expression vector,
215 similar to the one we report here, to produce secretary antibodies and succeeded in
216 obtaining functional monoclonal antibodies from SARS-CoV-2 infected individuals (28).
217 Collectively, our technology streamlines the isolation of mAbs for therapy and diagnosis.

218 Conclusion:

219 Our findings indicate that the developed antibody presentation system facilitates antibody
220 functional analysis and is well suited for the discovery of antibodies important for
221 infectious diseases when combined with conventional NGS-based antibody repertoire
222 analysis. Compared with droplet-based experimental systems, well-based systems are
223 limited in the number of cells they can process. Furthermore, experiments involving
224 infectious bacteria and viruses have imposed limitations on human experimentation. To
225 solve these problems, the automation of experiments will become important in the future.

226 By combining our screening system with robotic automation of experiments, it will be
227 possible to obtain useful mAbs for various diseases quickly and in large quantities, which
228 has broad implications for the development of vaccines against various diseases.

229 Materials and Methods:

230 Protein purification of influenza HAs (H1 and H2) as antigens

231 A mixture of 25.7 μg of HA, comprising H1 strain A/Puerto Rico/8/1934 (PR8), H1 strain
232 A/California/7/2009 (X-179A), H2 strain A/Okuda/1957 (H2), H3 strain A/Texas/50/2012
233 (X-223), or H5 strain A/Egypt/N03072/2010], 1.3 μg of NA (Strain-matched), and 3 μg of
234 BirA-expressing plasmids were transfected into Expi293 cells using the Expifectamine 293
235 transfection kit (Thermo Fisher Scientific, Waltham, MA, USA) according to the
236 manufacturer's instructions. The cells were then cultured in Expi293 Expression Medium
237 (Thermo Fisher Scientific) supplemented with D-biotin at a final concentration of 100 μM
238 for *in-vivo* BirA biotinylation in a humidified incubator containing 8% CO_2 at 37 °C and 125
239 rpm. If biotinylation was not necessary, transfection was performed without BirA, and cell
240 culture was carried out without D-biotin. Culture supernatants were harvested 3 days
241 post-transfection and filtered through a 0.45-μm filter (Merck Millipore, Burlington, MA,
242 USA). All proteins were purified with a Talon metal affinity resin (Takara Bio USA,

243 Mountain View, CA, USA) and dialyzed against pyrogen-free PBS. The oligomeric state and
244 purity were determined at 25 °C by size-exclusion chromatography on a Superdex 200
245 10/300GL column (GE Healthcare Technologies, Chicago, IL).

246 HA (H1 and H2) protein immunization

247 Two BALB/c mice were intraperitoneally immunized sequentially, 2 weeks apart, with 15
248 μg of H1 (PR8) HA, followed by 15 μg of H2 HA protein as an antigen and supplemented
249 with AddaVax adjuvant (InvivoGen, San Diego, CA, USA). Two weeks after the second
250 immunization, the mice were sacrificed, and their splenocytes were used for the
251 experiment. BALB/c mice were purchased from CLEA Japan (CLEA Japan, Inc., Tokyo,
252 Japan). All animal experiments were performed using protocols approved by the
253 Institutional Animal Care and Use Committee (IACUC) of the RIKEN Yokohama Branch.

254 Fluorescence-activated cell sorting

255 Using ACK (Ammonium-Chloride-Potassium) lysing buffer-treated splenocytes, CD43-
256 negative B cells were collected using AutoMACS (Miltenyi Biotec, Inc., Bergisch Gladbach,
257 North Rhine-Westphalia, Germany) and stained with IgG1 (Bv510), non-biotinylated His-
258 tagged purified recombinant His-tagged H1 (PR8) protein, and CD38 (PE-Cy7) on ice for
259 30 min. After washing three times, the cell suspension was incubated with Alexa Fluor

260 488-labeled anti-His antibodies on ice for 30 min. After washing three times, biotinylated
261 purified recombinant H2 protein was incubated on ice for 30 min. Furthermore after
262 washing three times, the cell suspension was incubated with Brilliant Violet 421-
263 conjugated streptavidin on ice for 3 min. We used 7-AAD for excluding dead cells. Next,
264 the B cells were subjected to single-cell sorting using a BD FACSAria III (BD Biosciences,
265 Franklin Lakes, NJ, USA) and collected into 96-well plates pre-loaded with lysis buffer. The
266 single cells in the lysis buffer were immediately snap-frozen on powdered dry ice and
267 stored at −80 °C.

268 Amplification of a paired B-cell repertoire amplicon from a single cell

269 Single cells were dropped into pre-loaded plates containing 4 μL/well of lysis buffer (2
270 U/μL RNase inhibitor, 0.5× PBS, 10 mM DTT) and 1 μL of 10 μM Oligo(dT)18 Primer. Cell
271 lysates were incubated at 70 °C for 90 s, followed by incubation at 35 °C for 15 s, and
272 then placed on ice for 2 min. For first-strand cDNA synthesis, 5 μL of RT mix (2× PCR
273 buffer, 5 mM DTT, 2 mM dNTP Mix, 10 U RNase inhibitor, 100 U SuperScript III Reverse
274 Transcriptase) was added to the cell lysate and incubated consecutively at 35 °C for 5
275 min, 45 °C for 20 min, 70 °C for 10 min, and 4 °C for chilling. For primer digestion, 5 μL
276 of the primer digestion mix (1× ExoI Buffer, 7.5 U Exonuclease I) was prepared and
277 incubated at 37 °C for 30 min, 80 °C for 20 min, and 4 °C for chilling. For the poly-A

278 tailing reaction, 5 μL of the poly-A tailing reaction mix (4× PCR buffer, 5 mM dATP, 0.1 U
279 RNase H, 60 U Terminal transferase) was prepared and incubated at 37 °C for 50 s, 65 °C
280 for 10 min, and 4 °C for chilling. For the 2nd strand cDNA synthesis, 25 μL of the
281 amplification mix (1× KAPA HiFi HotStart ReadyMix, 400 nM SMART_dT primer, 10 μL of
282 poly-A tailing product, 1.5 μL of nuclease-free H_2O) was prepared and incubated at 95 °C
283 for 3 min, 40 °C for 1 min, 65 °C for 10 min, and 72 °C for 5 min and chilled. For the
284 cDNA amplification using an Ig-specific outer primer set, 20 μL of the outer amplification
285 mix (1× KOD FX Neo buffer, 400 μM dNTPs, 1× UPM, 300 nM outer primer, 3.5 μL of the
286 SMART product, 0.5 U KOD FX Neo polymerase) was prepared and incubated at 94 °C for
287 2 min, followed by 25 cycles at 98 °C for 10 s, 60 °C for 30 s, and 68 °C for 45 s, and
288 then chilled. For cDNA amplification with an Ig-specific inner primer set, 20 μL of the inner
289 amplification mix (1× KOD FX Neo buffer, 400 μM dNTPs, 500 nM 5′ matrix primer mix,
290 500 nM 3′ matrix primer mix, 3.5 μL of the outer cDNA amplified product, 0.5 U KOD FX
291 Neo polymerase) was prepared and incubated at 94 °C for 2 min, followed by 25 cycles at
292 98 °C for 10 s, 60 °C for 30 s, and 68 °C for 45 s and then chilled. Finally, 3 μL of the
293 amplified inner cDNA product was used for further plate indexing by amplification. Then,
294 20 μL of the plate-indexing amplification mix (1× KOD FX Neo buffer, 400 μM dNTPs; 500
295 nM i5-Fwd or i7-Fwd, 500 nM i7-Rev or i5-Rev; 2 μL of the inner cDNA amplified product;
296 0.5 U KOD FX Neo polymerase) was prepared and incubated at 94 °C for 2 min, followed

297 by 25 cycles at 98 °C for 10 s, 60 °C for 30 s, and 68 °C for 45 s, and then chilled. All

298 primers used are listed in Supplementary Tables 1 and 2.

299 Paired-end Illumina sequencing strategy and analysis

300 The libraries were sequenced on a MiSeq instrument (Illumina, San Diego, CA, USA)

301 following the manufacturer's protocol. As the sequencing length was limited to 2 × 300

302 bp, we used the following strategy. Amplicons in both orientations were generated using

303 an Illumina adapter sequence. Then, asymmetric 400+100 nt paired-end sequencing was

304 performed to obtain high-quality 400 + 400 nt paired-end sequences of the original cDNA

305 molecule. This approach provided a sufficient sequencing length to capture extra-long Ig

306 variants. We followed the method by Turchaninova et al. (29). Only reads that met the

307 following four conditions were used as the resulting Ig sequences: 1) reads with a length

308 of 260 nt or more; 2) cumulative clustered reads representing the top 5% of the entire

309 reads; 3) 5'- and 3'-reads overlapping a length of 20 bases or more; and 4) a total length

310 of 460 ± 50 bp for heavy chain or 390 ± 40 bp for light chain. All resulting sequence data

311 were analyzed using IMGT/High V-QUEST (http://www.imgt.org/IMGT_vquest/vquest) for

312 annotation (30). Using the sequences and annotations, Ig database construction and

313 visualization of the Ig repertoire were performed using the in-house BONSCI software.

314 ## Construction of a mouse IgG/IgK expression plasmid

315 The BsaI restriction sites were inserted into the paired B-cell repertoire amplicon from a
316 single cell using PCR. The destination vector contained the IL6 signal peptide, EF1a
317 promoter, ccdB gene, and mouse IgK Fc region. The donor vector contained the mouse
318 IgG1 Fc region, the *Venus* gene, and the EF1a promoter. The paired B-cell repertoire
319 amplicons, destination vector, and donor vector containing BsaI restriction sites were
320 assembled using our assembly method. For this step, 10 μL of the assembly mix (1× T4
321 DNA ligase buffer, 1× BSA, 1 U BsaI restriction enzyme, 40 U T4 DNA ligase, 100 ng
322 heavy chain amplicon, 100 ng light chain amplicon, 100 ng destination vector, and 100 ng
323 donor vector) was prepared and incubated for 25 cycles at 37 °C for 3 min, 16 °C for 4
324 min, 50 °C for 5 min, and 80 °C for 5 min, and then chilled. The antibody sequence that
325 entered the construct was fused to the *Venus* sequence and expressed in membrane form.

326 ## Antibody display on FreeStyle 293 cultured cells

327 One microgram of antibody-expressing plasmid was transfected into 1 x 10^6 FreeStyle 293
328 cells in 1-mL culture using the 293fectin Transfection Reagent (Thermo Fisher Scientific)
329 according to the manufacturer's instructions and cultured in FreeStyle 293 Expression
330 Medium (Thermo Fisher Scientific) in a humidified incubator with 8% CO_2 at 37 °C and
331 125 rpm. Antibodies were displayed on the surface of cultured cells, which enabled the

332 determination of antigen specificity. Furthermore, the antibody-display cells were tested
333 for binding activity with Alexa647-labeled H1 and Alexa568-labeled H2 (Alexa Fluor™
334 Antibody Labeling Kits, ThermoFisher Scientific) using a BD FACSAria III (BD Biosciences).

335 Antibody production

336 To obtain a large amount of secretory antibodies, PCR fragments from the antibody-
337 expressing plasmid were cloned into the pcDNA3.4-mIgG1 or pcDNA3.4-kappa vectors. A
338 mixture of 15 μg of pcDNA3.4-V-gene-mIgG1 vector and 15 μg of pcDNA3.4-V-gene-
339 kappa vector was transfected into Expi293 cells using the ExpiFectamine 293 Transfection
340 Kit (Thermo Fisher Scientific), according to the manufacturer's instructions, and cultured in
341 Expi293 Expression Medium (Thermo Fisher Scientific) in a humidified 8% CO_2 incubator at
342 37 °C and 125 rpm. Then, 5 days post-transfection, the culture supernatants were
343 harvested, and all proteins were purified with PureSpeed IMAC resin (Mettler Toledo,
344 Columbus, OH, USA), according to the manufacturer's instructions.

345 Surface plasmon resonance

346 Kinetic analyses were performed at 25 °C using a BIAcore 3000 machine (GE Healthcare
347 Technologies). A2p1, B10p2, C10p2, E11p2, G6p2, A6p4, D4p4, D11p4, or G12p4
348 antibodies were immobilized on a CM5 sensor chip (GE Healthcare Technologies) with an
349 amine-coupling kit according to the manufacturer's instructions. HA probes were serially

350 diluted at five different concentrations and injected at a flow rate of 30 μL/min for 3 min
351 with a dissociation time of 7 min in HBS–EP buffer (10 mM HEPES, pH 7.4, 150 mM NaCl,
352 3.4 mM EDTA, and 0.005% Surfactant P20). The chip was regenerated using 10 mM
353 glycine (pH 2.5) as an HA probe.

354

355 Data access:

356 All raw and processed sequencing data generated in this study have been submitted to the
357 NCBI Gene Expression Omnibus (GEO; https://www.ncbi.nlm.nih.gov/geo/) under
358 accession number GSE140720.

359 Acknowledgements:

360 We thank Mr. Atsuo Kobayashi, Ms. Chieko Okamura, Dr. Seok-Won Kim, Mr. Maxime
361 Hebrard, Dr. Todd D Taylor, and the RIKEN IMS Genome Platform for their technical
362 support, Dr. Atsushi Miyawaki for gifting the *Venus* gene, and Dr. Christopher Nicholas for
363 critical reading and English editing of the manuscript. We would like to thank Editage
364 (www.editage.jp) for English language editing.

Funding:

This study was supported in part by research grants from the RIKEN Research Program 'Single cell Project' (O.O., T.W., T.K., and H.F.) and Grants-in-Aid for Scientific Research (S) [26221306 to T.K. and H.F.]. The funding sources were not involved in the study design, data collection and interpretation, or paper submission decisions.

Conflict of interest:

None declared.

Author contributions:

Conceptualization: Takashi Watanabe, Hidehiro Fukuyama; Data curation: Yoshiki Mochizuki, Naveen Kumar; Formal analysis: Yoshiki Mochizuki, Naveen Kumar; Funding acquisition: Osamu Ohara, Tomohiro Kurosaki, Takashi Watanabe, Hidehiro Fukuyama; Investigation: Hikaru Hata, Fumie Yokoyama, Tomoko Hasegawa; Methodology: Takashi Watanabe, Hidehiro Fukuyama; Project administration: Takashi Watanabe, Hidehiro Fukuyama; Resources: Takashi Watanabe, Hidehiro Fukuyama; Software: Yoshiki Mochizuki, Naveen Kumar; Supervision: Osamu Ohara, Tomohiro Kurosaki; Validation: Takashi Watanabe, Hidehiro Fukuyama; Visualization: Takashi Watanabe, Hidehiro Fukuyama; Writing – original draft: Takashi Watanabe, Hidehiro Fukuyama; Writing–review & editing: Takashi Watanabe, Hidehiro Fukuyama.

383 # References:

384 1. Balsitis, S. J., K. L. Williams, et al. (2010). Lethal antibody enhancement of dengue
385 disease in mice is prevented by Fc modification. *PLoS Pathog.,* **6**(2): e1000790.
386 2. Fang, X. T., D. Sehlin, et al. (2017). Efficient and inexpensive transient expression of
387 multispecific multivalent antibodies in Expi293 cells. *Biol. Proced. Online,* **19**(1): 1–9.
388 3. Köhler, G. and C. Milstein (1975). Continuous cultures of fused cells secreting antibody
389 of predefined specificity. *Nature*, **256**(5517): 495–497.
390 4. Traggiai, E., S. Becker, et al. (2004). An efficient method to make human monoclonal
391 antibodies from memory B cells: potent neutralization of SARS coronavirus. *Nat. Med*.,
392 **10**(8): 871–875.
393 5. Kwakkenbos, M. J., S. A. Diehl, et al. (2010). Generation of stable monoclonal
394 antibody-Producing B cell receptor-positive human memory B cells by genetic
395 programming. *Nat. Med*., **16**(1): 123–128.
396 6. Wrammert, J., K. Smith, et al. (2008). Rapid cloning of high-affinity human monoclonal
397 antibodies against influenza virus. *Nature*, **453**(7195): 667–671.
398 7. Meijer, P. J., P. S. Andersen, et al. (2006). Isolation of human antibody repertoires
399 with preservation of the natural heavy and light chain pairing. *J. Mol. Biol.*, **358**(3):
400 764–772.

401 8. Kuraoka, M., A. G. Schmidt, et al. (2016). Complex antigens drive permissive clonal
402 selection in germinal centers. *Immunity*, **44**(3): 542–552.
403 9. Clackson, T., H. R. Hoogenboom, et al. (1991). Making antibody fragments using
404 phage display libraries. *Nature*, **352**(6336): 624–628.
405 10. Feldhaus, M. J., R. W. Siegel, et al. (2003). Flow-cytometric isolation of human
406 antibodies from a nonimmune Saccharomyces cerevisiae surface display library. *Nat.*
407 *Biotechnol.*, **21**(2): 163–170.
408 11. Harvey, B. R., G. Georgiou, et al. (2004). Anchored periplasmic expression, a versatile
409 technology for the isolation of high-affinity antibodies from Escherichia coli-expressed
410 libraries. *Proc. Natl. Acad. Sci. U. S. A.*, **101**(25): 9193–9198.
411 12. Schaffitzel, C., J. Hanes, et al. (1999). Ribosome display: an in vitro method for
412 selection and evolution of antibodies from libraries. *J. Immunol. Methods*, **231**(1–2):
413 119–135.
414 13. Mazor, Y., T. Van Blarcom, et al. (2007). Isolation of engineered, full-length antibodies
415 from libraries expressed in Escherichia coli. *Nat. Biotechnol.*, **25**(5): 563–565.
416 14. Kubota-Koketsu, R., H. Mizuta, et al. (2009). Broad neutralizing human monoclonal
417 antibodies against influenza virus from vaccinated healthy donors. *Biochem. Biophys.*
418 *Res. Commun.*, **387**(1): 180–185.
419 15. Setliff, I., A. R. Shiakolas, et al. (2019). High-throughput mapping of B cell receptor

420 sequences to antigen specificity. *Cell*, **179**(7): 1636–1646. e15.

421 16. Kirchmaier, S., K. Lust, et al. (2013). Golden GATEway cloning--a combinatorial

422 approach to generate fusion and recombination constructs. *PloS One*, **8**(10): e76117.

423 17. Okuno, Y., Y. Isegawa, et al. (1993). A common neutralizing epitope conserved

424 between the hemagglutinins of influenza A virus H1 and H2 strains. *J. Virol.*, **67**(5):

425 2552–2558.

426 18. Ekiert, D. C., A. K. Kashyap, et al. (2012). Cross-neutralization of influenza A viruses

427 mediated by a single antibody loop. *Nature*, **489**(7417): 526–532.

428 19. Impagliazzo, A., F. Milder, et al. (2015). A stable trimeric influenza hemagglutinin stem

429 as a broadly protective immunogen. *Science*, **349**(6254): 1301–1306.

430 20. Nagai, T., K. Ibata, et al. (2002). A variant of yellow fluorescent protein with fast and

431 efficient maturation for cell-biological applications. *Nat. Biotechnol.*, **20**(1): 87–90.

432 21. D'Angelo S, Ferrara F, et al. (2018). Many Routes to an Antibody Heavy-Chain CDR3:

433 Necessary, Yet Insufficient, for Specific Binding. *Front. Immunol.*, **9**(395)

434 22. Xu, J. L. and M. M. Davis (2000). Diversity in the CDR3 region of VH is sufficient for

435 most antibody specificities. *Immunity*, **13**(1): 37–45.

436 23. Gamblin, S. J., and J.J. Skehel. (2010). Influenza hemagglutinin and neuraminidase

437 membrane glycoproteins. *J. Biol. Chem.*, **285**(37): 28403–28409.

438 24. Adachi, Y., T. Onodera, et al. (2015). Distinct germinal center selection at local sites
439 shapes memory B cell response to viral escape. *J. Exp. Med.*, **212** (10): 1709–1723.
440 25. Kaplon H, Crescioli S, et al. (2023). Antibodies to watch in 2023. *Mabs*, **15**(1):
441 2153410
442 26. Soni P, A Yasuhara, et al. (2018). Evaluation of the fusion partner cell line SPYMEG for
443 obtaining human monoclonal antibodies against influenza B virus. *J. Vet. Med. Sci.*,
444 **80**(6): 1020–1024
445 27. Petropoulos, K., (2012) Phage display. *Methods Mol. Biol.*, **901**: 33–51.
446 28. Lima, N. S., M. Musayev, et al. (2022). Primary exposure to SARS-CoV-2 variants
447 elicits convergent epitope specificities, immunoglobulin V gene usage and public B cell
448 clones. *Nat. Commun.*, **13**(1): 7733.
449 29. Turchaninova, M. A., A. Davydov, et al. (2016). High-quality full-length
450 immunoglobulin profiling with unique molecular barcoding. *Nat. Protoc.*, **11**(9): 1599–
451 1616.
452 30. Alamyar, E., P. Duroux, et al. (2012). IMGT® tools for the nucleotide analysis of
453 immunoglobulin (IG) and T cell receptor (TR) V-(D)-J repertoires, polymorphisms, and
454 IG mutations: IMGT/V-QUEST and IMGT/HighV-QUEST for NGS. *Methods Mol. Biol.*,
455 **882**: 569–604.
456

457 # Figures:

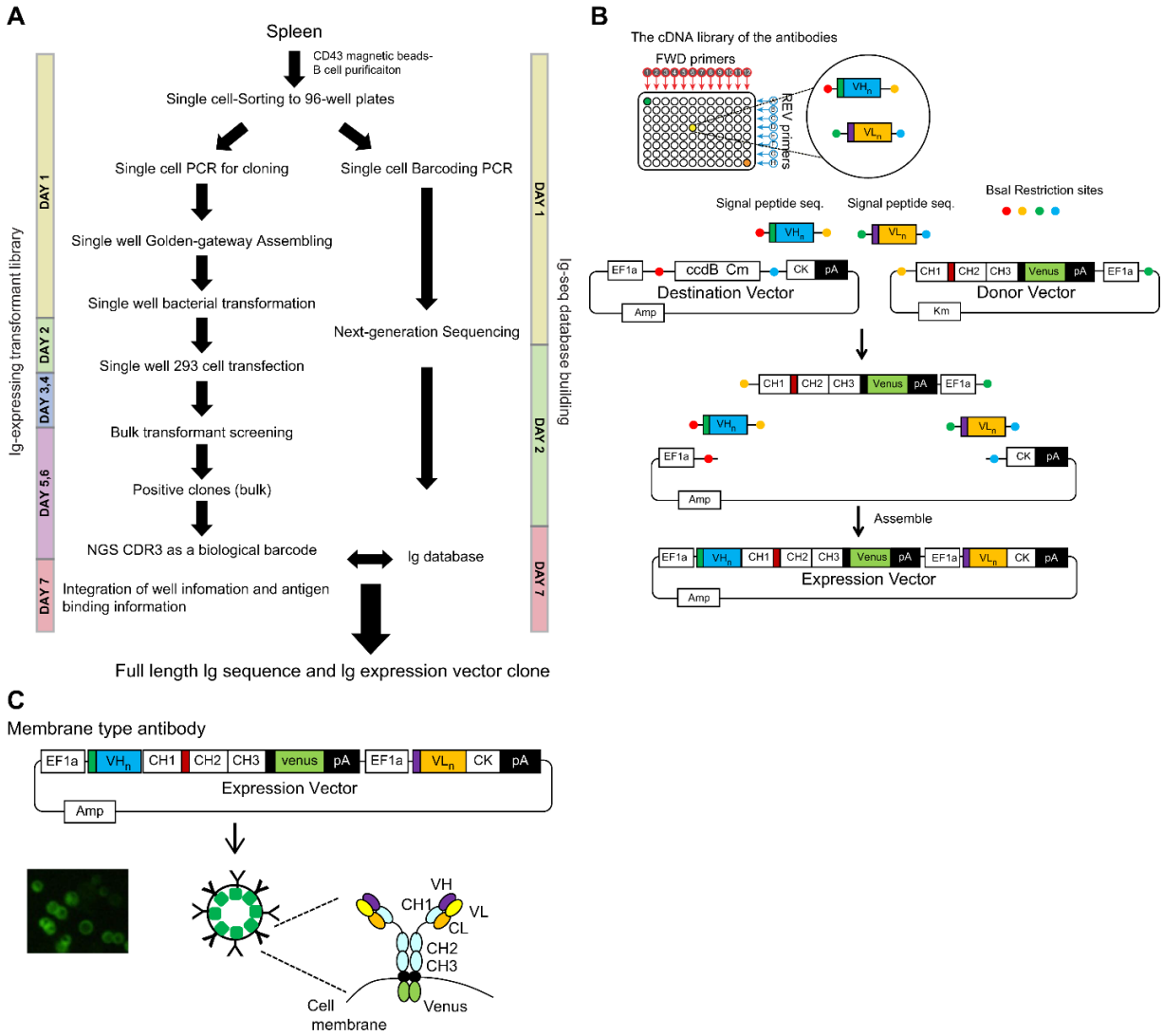

458

459 **Figure 1.** System to link the antigen-binding feature with the Ig repertoire genetic

460 information. **A.** Single cell-sorted B cells were subjected to two processes: Ig-seq database

461 building and Ig-expressing transformant library preparation. Antigen-binding Ig

462 transformants were collected by sorting in bulk and the sequences of the unique CDR3

463 regions and clones of interest were identified by referring to the Ig-seq database. The

464 duration of each steps are indicated. **B.** To express both Ig heavy and kappa/lambda

465 chains in a single-expression vector, we generated a dual-expression vector. Four gene

466 fragments were assembled by the Golden Gate method using the BsaI restriction enzyme.

467 They included: 1) the destination vector containing the Ig kappa constant gene and the

468 ccdB Chloramphenicol cassette for negative selection, 2) fragments containing the Ig

469 heavy constant gene fused to *Venus* derived from the donor vector, 3) the Ig heavy

470 variable gene fragment, and 4) the Ig light variable gene fragment. **C.** Individually purified

471 plasmids were transiently transfected to the floating human FreeStyle 293 cell line. Igs

472 were expressed on the cell surface in 2 days, and expression levels were confirmed and

473 normalized by *Venus* expression, since the Ig heavy chain was fused to *Venus* at the

474 cytoplasmic domain tail.

475

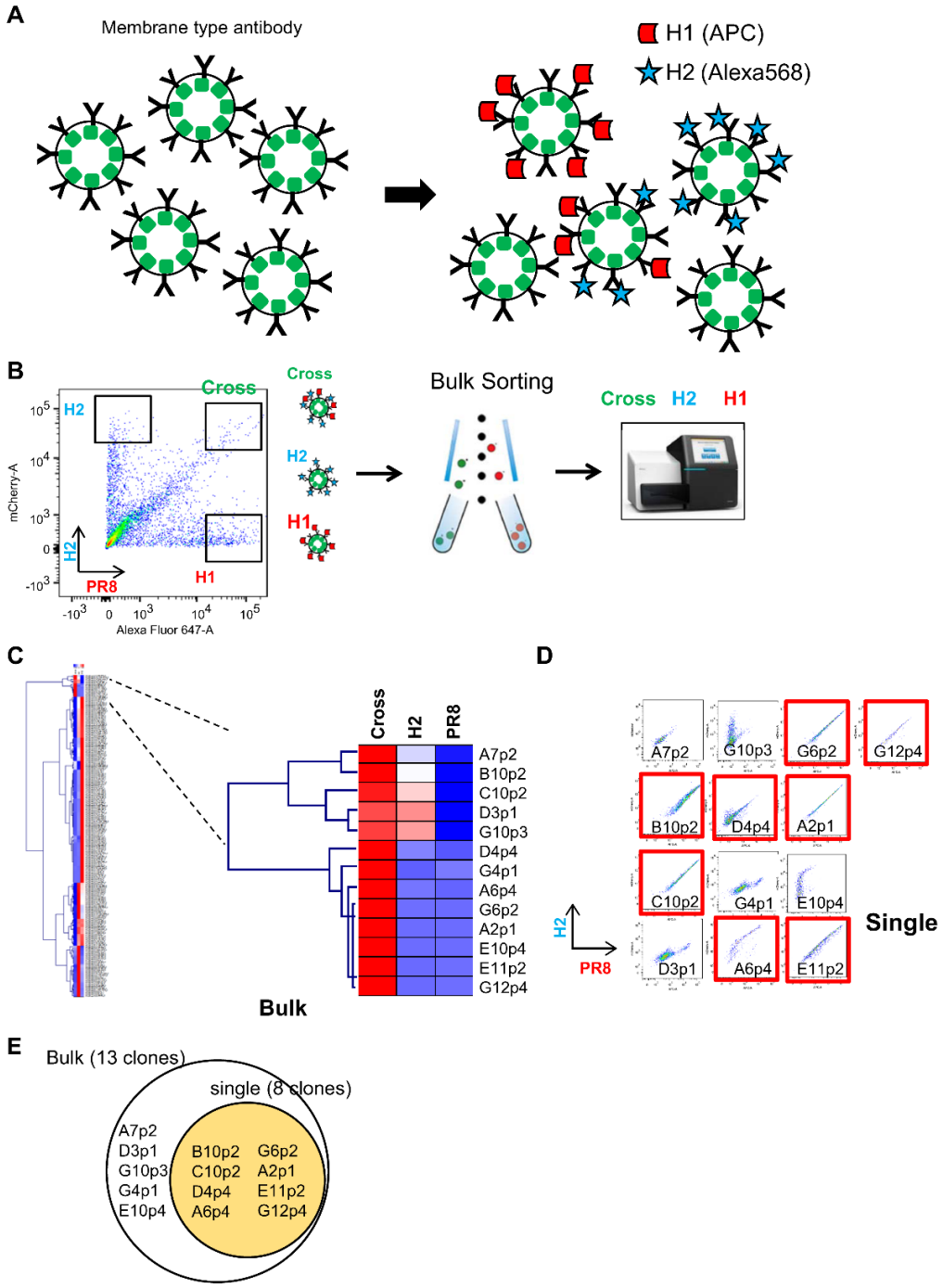

Figure 2. Isolation of H2 and H1-reactive B cells. **A.** Mixture of Ig-expressing transformant libraries stained with HA probes. **B.** Three strong HA-binding populations, $H1^{+}H2^{+}$ (cross), $H2^{+}$ (H2), and $H1^{+}$ (H1), were sorted and collected in a bulk fashion. Then, these three

480 collected populations were and sequenced. **C.** The bulk Ig-seq data were referred to as the

481 single-cell Ig-seq data. Heatmap indicates the appearance rate of individual clone in each

482 box shown in B (H1, H2, or Cross) among sorted 2,981 cells of mixture of 190 clone

483 transformants. $H1^{+}H2^{+}$ (cross) clones are shown on the right columns. High to low

484 appearance rate reflects red to blue color. **D.** The individual flow cytometry profile of 13

485 "Cross" transformants obtained by the bulk examination are shown and red labeled ones

486 are also found by the individual examination(red). **E.** A summary of the results in

487 comparison of the bulk and individual examination methods.

488

489

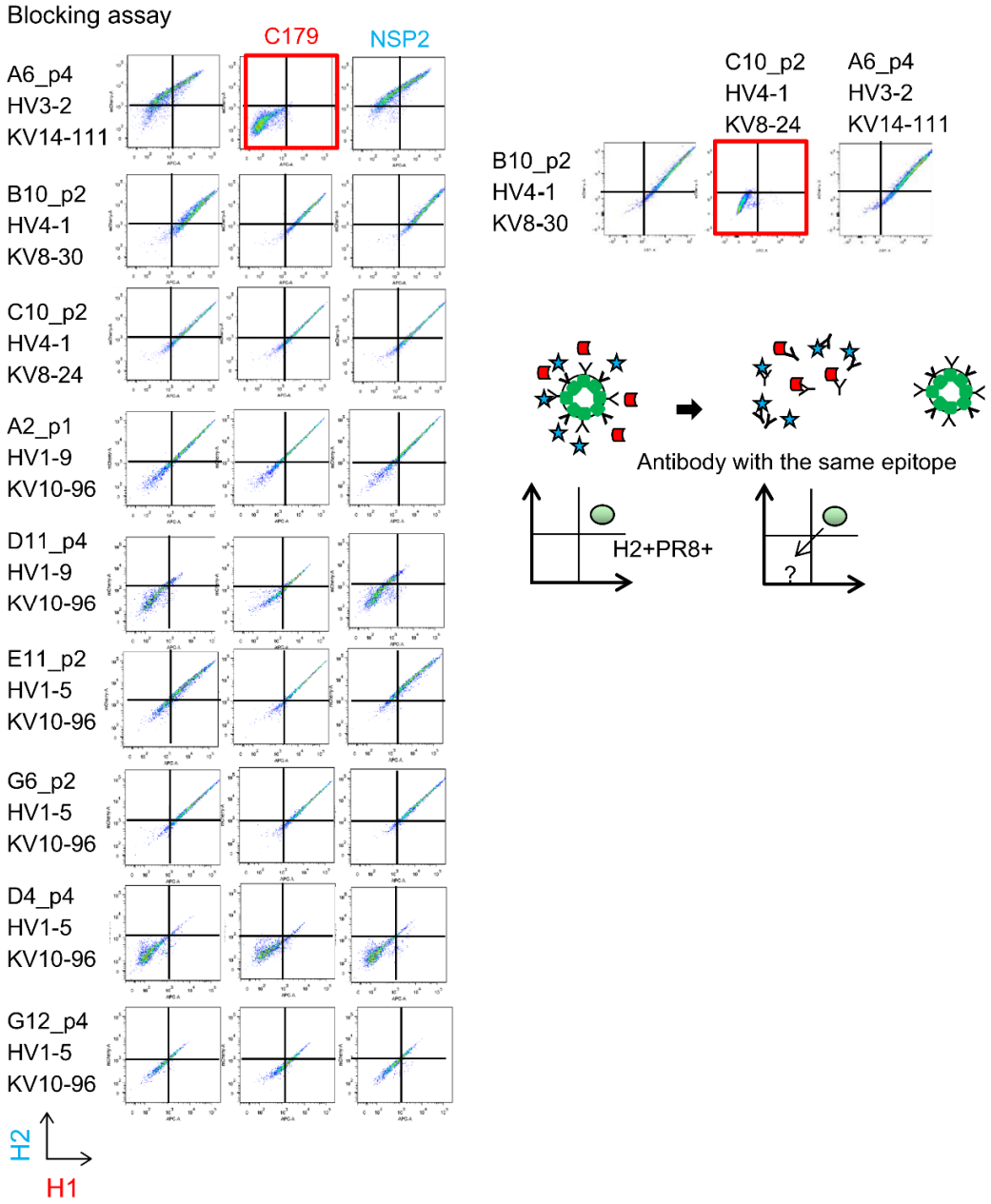

490

491 **Figure 3.** Competition assay of "cross" Ig-transformants using C179, a broadly-reactive

492 mAb binding to the Stem region of HA, and NSP2 (Narita strain-specific mAb), a strain-

493 specific mAb that binds to the head region of HA. On the right panel, two stem-reactive

494 clones (see Table 1) were examined reciprocally with combination of transformant and

495 recombinant antibodies.

496

Table 1

Table 1. Affinities (K_d) of the antibodies to six HA antigens from strains A/Okuda/1957(H2N2), termed H2, A/Puerto Rico/8/1934(H1N1), termed PR8, A/California/2009 (X-179A) [H1N1] Pdm09, termed Cal, A/Texas/50/2012 (X-223) [H3N2], termed H3, A/Egypt/N03072/2010(H5N1), termed H5, and A/Brisbane/59/2007 (H1N1), termed Stem, were determined using surface plasmon resonance analysis. H2, PR8, Cal, and H5 belong to group 1, and H3 belongs to group 2.

Group	1	1	1	2	1	1
	H2	**PR8**	**Cal**	**H3**	**H5**	**Stem**
A6p4	4.51E-08	1.41E-06	1.14E-05		2.91E-05	1.59E-08
B10p2	6.75E-09	2.3E-09	3.29E-09			
C10p2	1.66E-09	1.29E-09	5.66E-10			4.26E-08
A2p1	2.49E-06	1.42E-07	1.14E-05	1.25E-04	1.91E-05	
D11p4	7.93E-07	1.72E-06	1.04E-06	1.36E-05	1.05E-11*	
E11p2	4.4E-08	1.86E-08	1.67E-06	2.92E-07	2.37E-07	
G6p2	3.51E-08	3.53E-08	1.44E-08	1.78E-05	3.05E-08	
D4p4	1.1E-05	1.78E-05	6.4E-05	4.38E-05	2.47E-05	
G12p4	1.45E-07	1.52E-07	5.7E-07	9.44E-07	1.58E-07	

* The affinity of D11p4 for H5 was low and inaccurate (Supplementary Figure 2).

Surface plasmon resonance (Biacore) KD (M)

High
Middle
Low

516 # Supplementary Tables

517 **Supplementary Table 1. Oligonucleotides**

Primer	Application	Sequence
First-strand cDNA synthesis		
Oligo(dT)18	Primer for cDNA synthesis	TTTTTTTTTTTTTTTTTT
Second-strand cDNA synthesis		
SMART_dT	TdT oligo	AAGCAGTGGTATCAACGCAGAGTAC$(T)_{30}$VN
Mouse IGH/IGK primer		
TdT_L_BsaI_heavy	mouse IgG heavy-chain cDNA	CTAGGGTCTCAAGCAGTGGTATCAACGCAGAGTAC
msVHE		GAGGTGCAGCTGCAGGAGTCTGG
W-gamma-outer		AGAAGGTGTGCACACCGCTGGAC
mC_G new2		ATCTCCACACACAGGGGCCAGTGGATAGAC
BsaI_IL6sp_L		CTAGGGTCTCAAGCAGATGAACTCCTTCTCCACAAGCG
mC_G_new2_BsaI		TCCTAGGTCTCCCACACACAGGGGCCAGTGGATAGAC
TdT_L_BsaI_light	mouse IgK light-chain cDNA	CTAGGGTCTCAGTGGTATCAACGCAGAGTAC
mvkappa		GAYATTGTGMTSACMCARWCTMCA
mCkappa-outer		ACTGAGGCACCTCCAGATGTT
mC_K_new		AGGCACCTCCAGATGTTAACTGCTCACTGG
BsaI_IL6sp_kappa_L		CTAGGGTCTCAGTGGTATGAACTCCTTCTCCACAAGCG
mC_K_new_BsaI		TCCTAGGTCTCCTCCAGATGTTAACTGCTCACTGG

518

519

520 **Supplementary Table 2. Oligonucleotides**

Primer	Application	Sequence
Next Generation sequencing		
M13fwd_i5_mC_G_new2[a]	Well index	TGTAAAACGACGGCCxxxxxxxxATCTCCACACACAGGGGCCAGTGGATAGAC
M13fwd_i5_mC_K[a]		TGTAAAACGACGGCCxxxxxxxxGCACCTCCAGATGTTAACTG
M13fwd_i5_mC_L[a]		TGTAAAACGACGGCCxxxxxxxxAGCTCCTCAGRGGAAGGTG
M13rev_i7_msVHE[b]		GGAAACAGCTATGACyyyyyyyyGAGGTGCAGCTGCAGGAGTCTGG
M13rev_i7_mvkappa[b]		GGAAACAGCTATGACyyyyyyyyGAYATTGTGMTSACMCARWCTMCA
i5-Fwd[c]	Plate index	AATGATACGGCGACCACCGAGATCTACACxxxxxxxxACACTCTTTCCCTACACGACGCTCTTCCGATCTTGTAAAACGACGGCC
i7-Rev[d]		CAAGCAGAAGACGGCATACGAGATyyyyyyyyGTGACTGGAGTTCAGACGTGTGCTCTTCCGATCTGGAAACAGCTATGAC
i5-Rev[c]		AATGATACGGCGACCACCGAGATCTACACxxxxxxxxACACTCTTTCCCTACACGACGCTCTTCCGATCTGGAAACAGCTATGAC
i7-Fwd[d]		CAAGCAGAAGACGGCATACGAGATyyyyyyyyGTGACTGGAGTTCAGACGTGTGCTCTTCCGATCTTGTAAAACGACGGCC

521 [a]xxxxxxxx: sequence showing the well index from D501 to D508. [b]yyyyyyyy: sequence
522 showing the well index from D701 to D712. [c]xxxxxxxx: sequence showing the plate index
523 from D501 to D508. [d]yyyyyyyy: sequence showing the plate index from D701 to D712.
524

Supplementary Figures

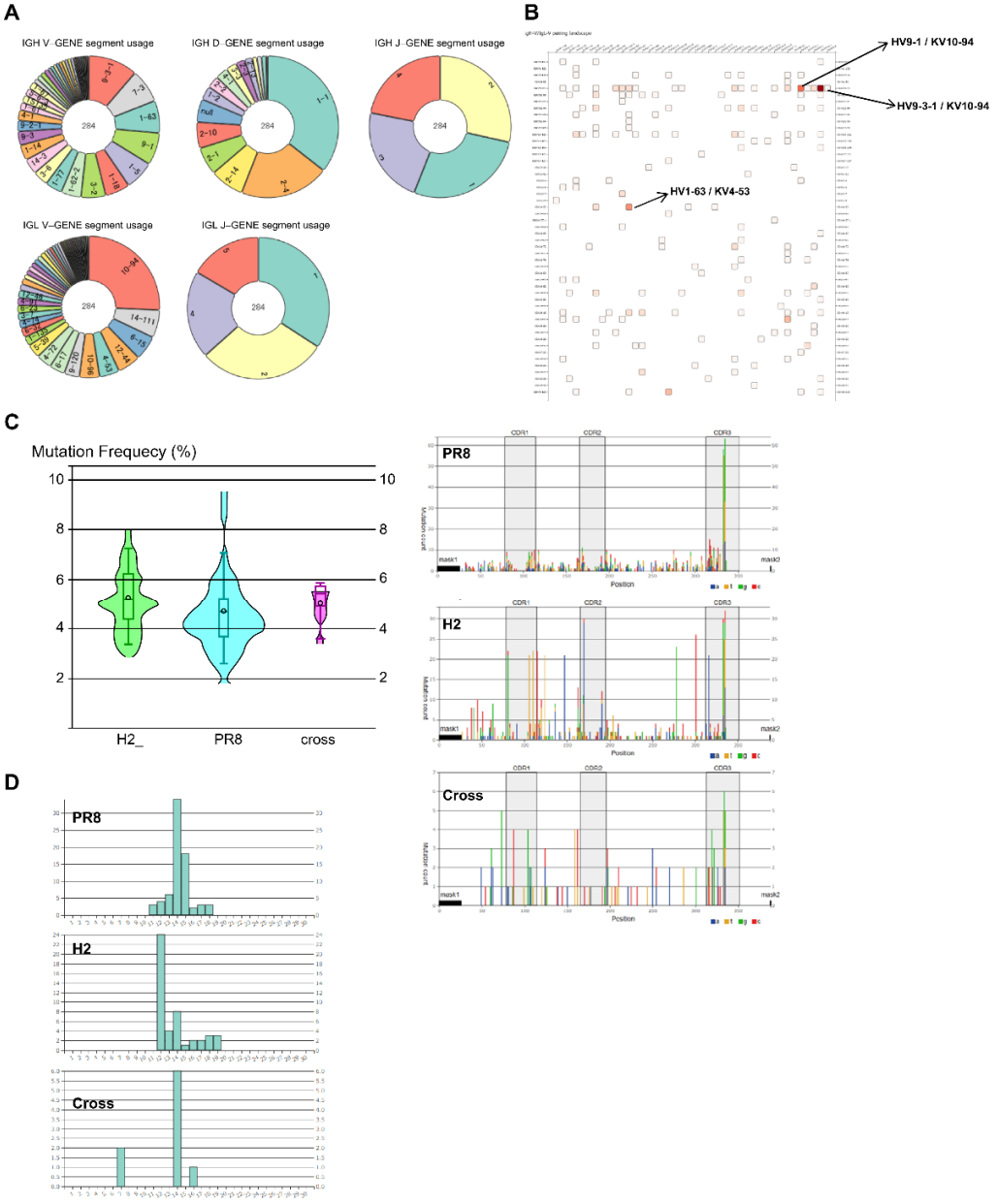

Supplementary Figure 1.

The Ig repertoires are visualized using the in-house software. Overview of heavy (V-D-J) and light (V-J) chain usages (**A**), and the repertoire clonality (**B**) is shown. (**C**) The mutation rates and their positions of heavy chains in three cell populations (PR8+, H2+, PR8+H2+) are compared. (**D**) The lengths of CDR3 of heavy chains of three cell populations (PR8+, H2+, PR8+H2+) are compared.

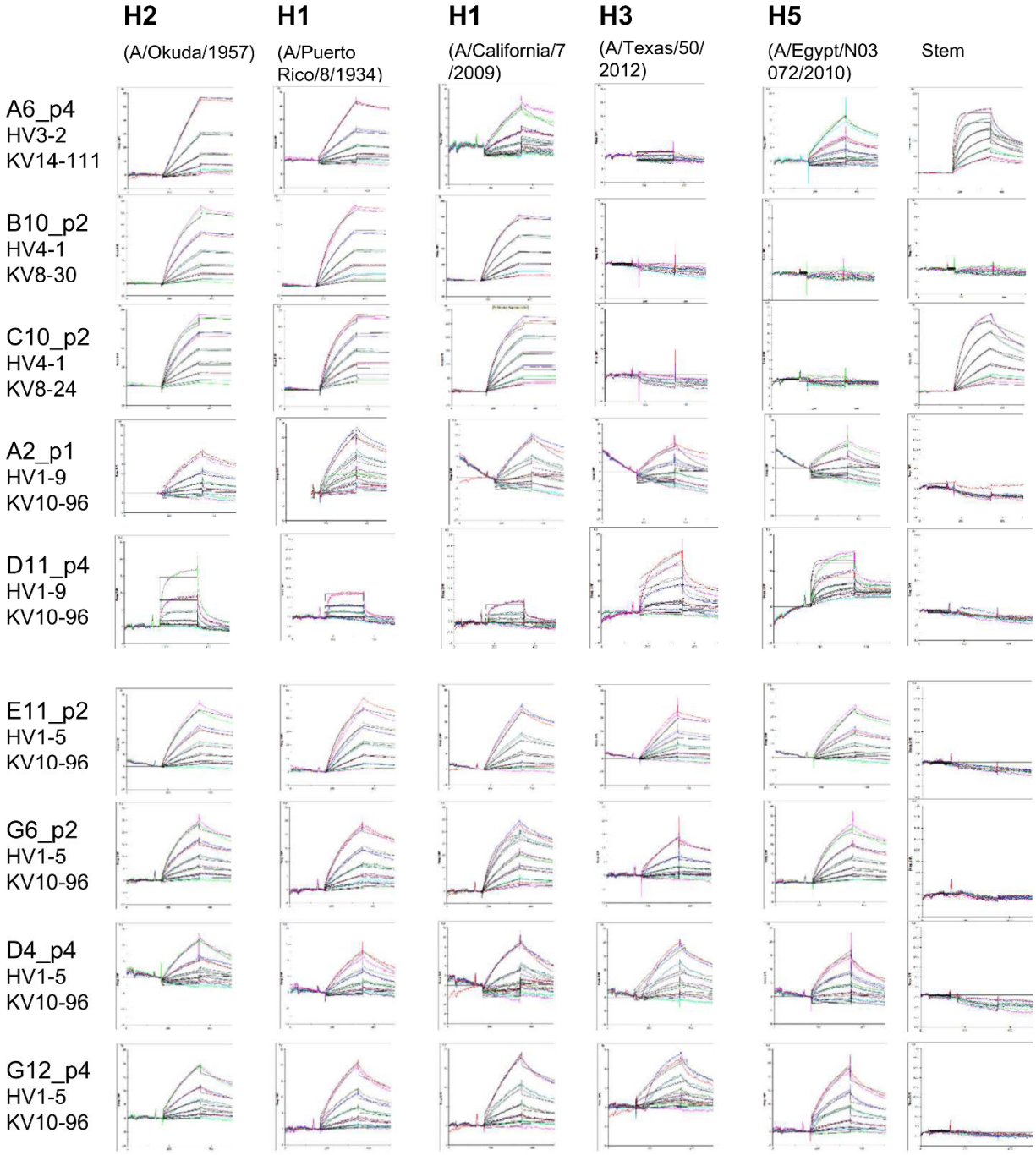

Supplementary Figure 2.

SPR profiles of kinetics analysis of nine clones, A6p4, B10p2, C10p2, A2p1, D11p4, E11p2, G6p2, D4p4, and G12p4 using a BIAcore 3000 machine (GE Healthcare).

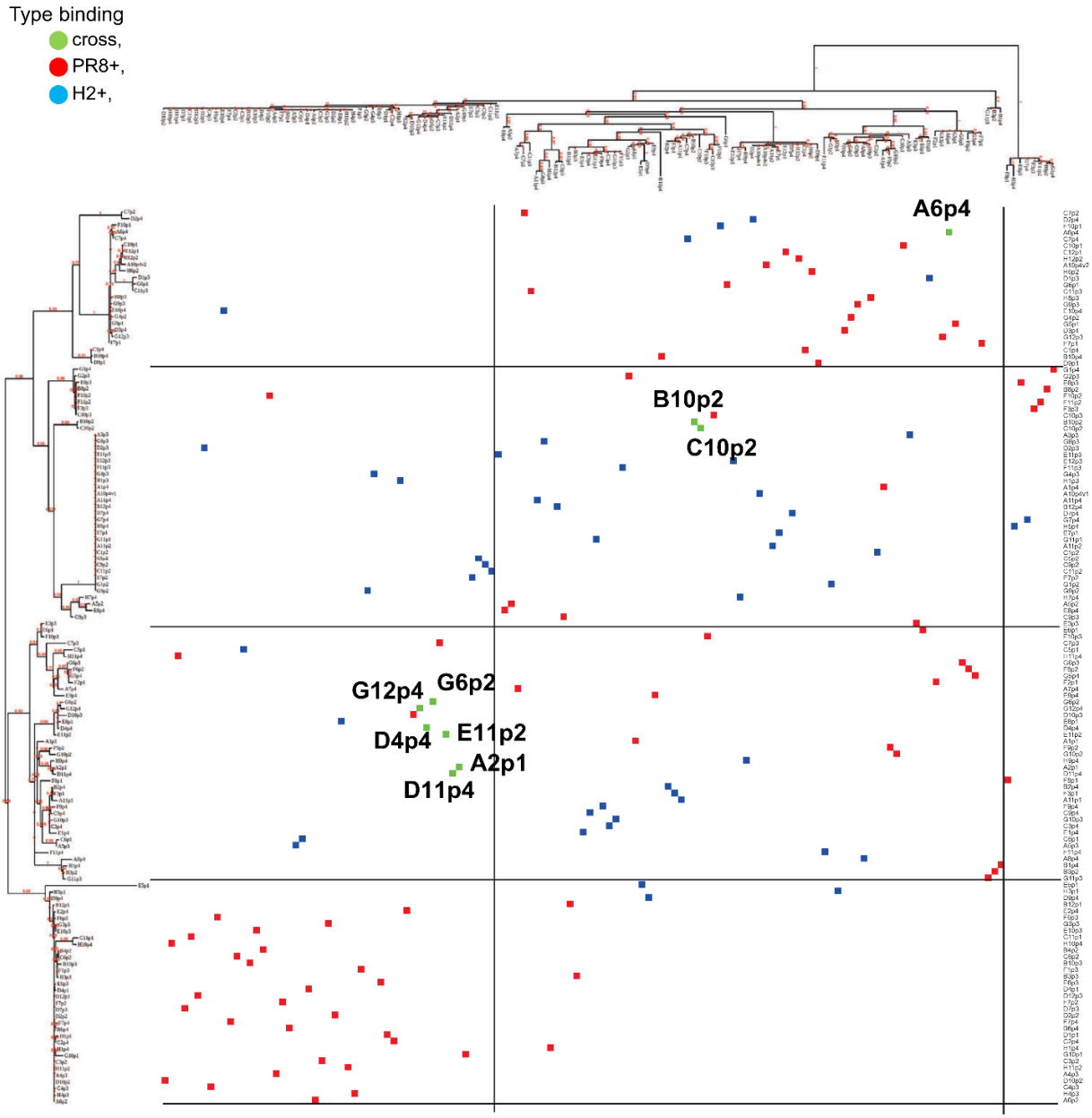

Supplementary Figure 3.

Two hundred and eighty-four clones are plotted in a two-dimensional map of phylogeny trees for heavy and light chain genes. Nine mAb clones are overlaid in green. Six “cross” clones are located in a major cluster. B10p2 and C10p2 are co-localized and distant from the cluster. A6p4 is uniquely located in the map.

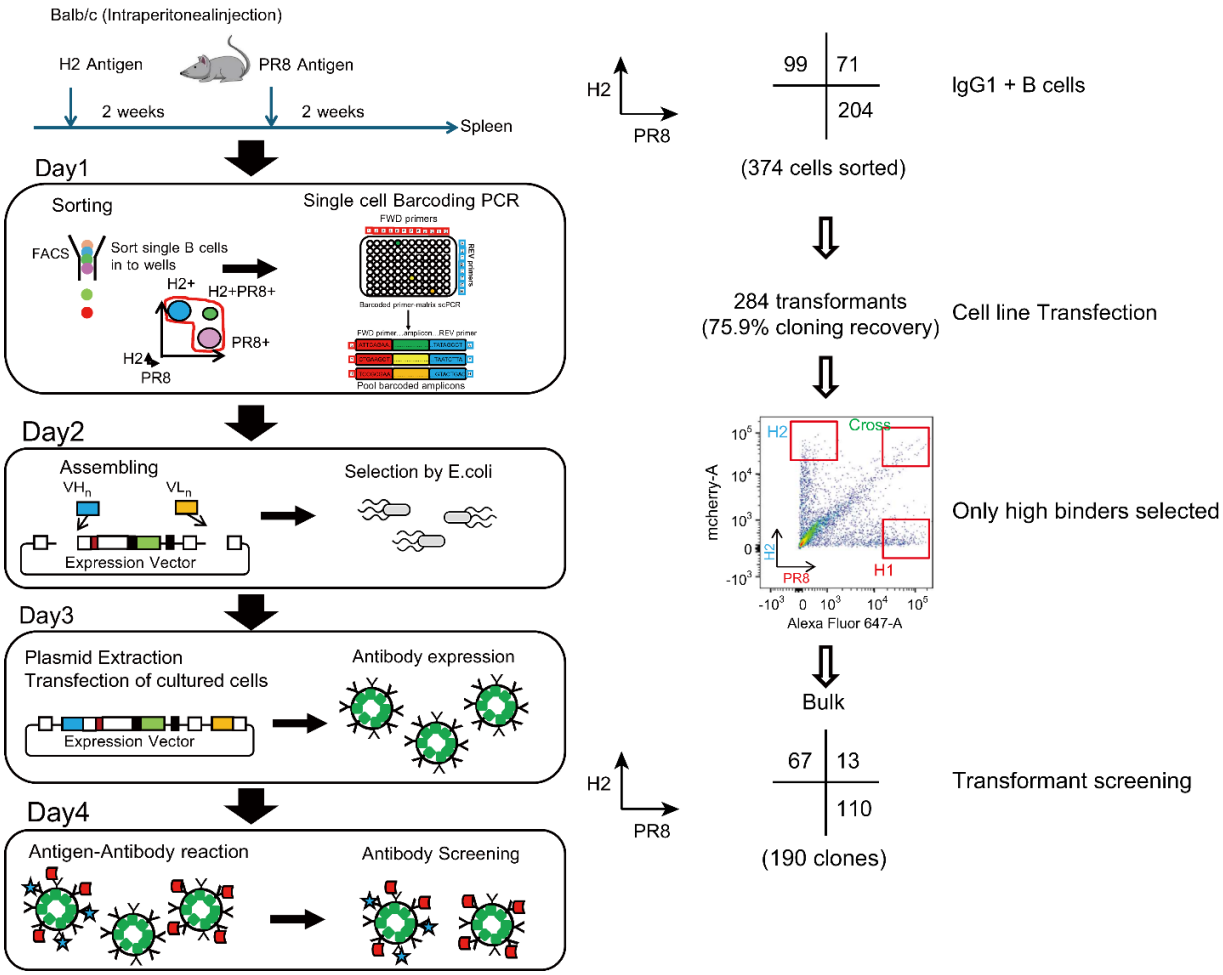

Supplementary Figure 4.

Progression Flowchart. The process for efficiently isolating influenza cross-reactive antibodies from mouse germinal center B cells with high affinity is shown. Experiment outcome flow numbers of clones in each step are indicated.

553

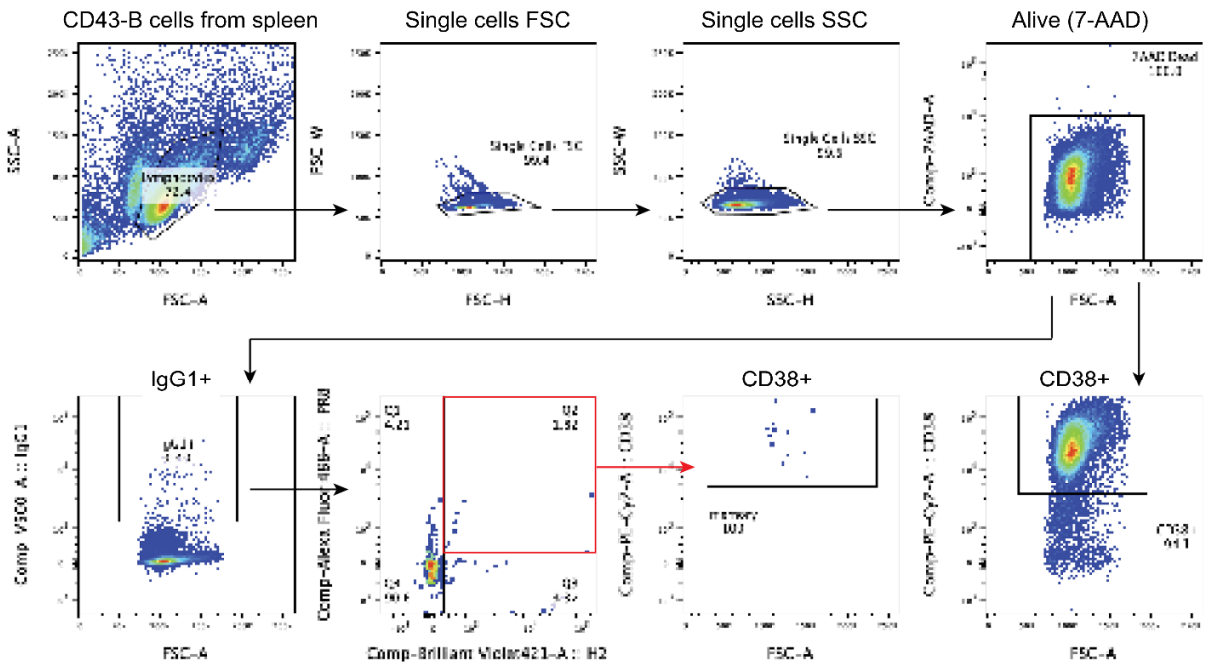

Sorting strategy MACS beads negatively purified B cells from the spleen are sorted for IgG1+ cells and then separated with H2 and PR8. The majority of cross-reactive IgG1+ cells(red box) are CD38+ cells, most likely in memory compartment. For the reference, the CD38 staining pattern of total live B cells in shown at the bottom right.

554

555 **Supplementary Figure 5.**

556 Sorting strategy. CD43 MACS B cells from the spleen purified using negatively charged
557 beads were sorted for IgG1+ cells and then separated into H2 and PR8. The majority
558 of cross-reactive IgG1+ cells (red box) were CD38+ cells, most likely in the memory
559 compartment. For reference, the CD38 staining pattern of total live B cells is shown at
560 the bottom right.

561

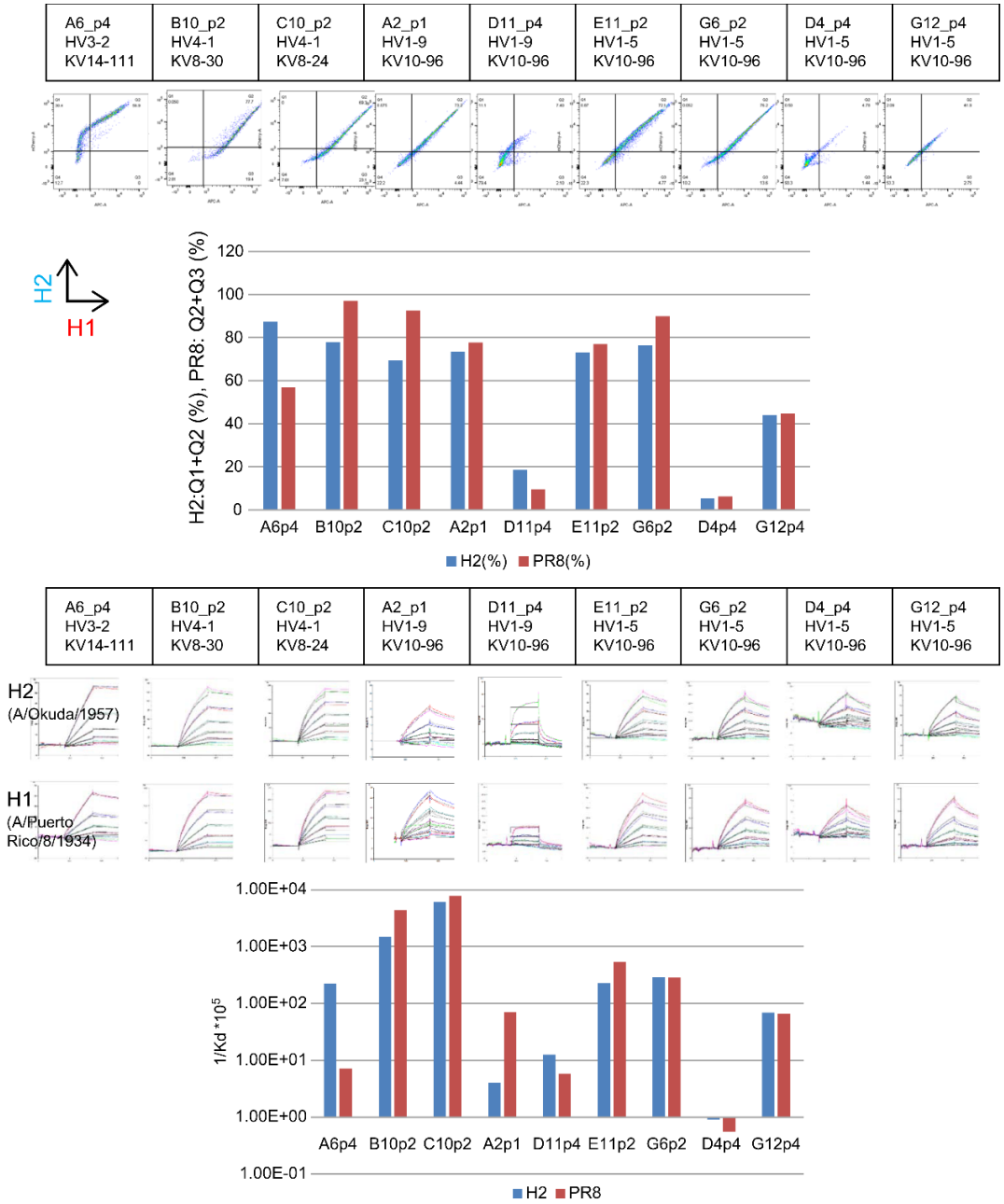

Supplementary Figure 6.

The affinity of antigen-antibody binding (in this case, probe and membrane-bound antibody expressing cell) can be inferred from the population shift (flow cytometry analysis).